AQUA
Water Infrastructure, Ecosystems and Society

IWA PUBLISHING

 AQUA — Water Infrastructure, Ecosystems and Society Vol 71 No 10, 1180 doi: 10.2166/aqua.2022.089

Detecting land surface water changes in the Upper Mzingwane sub-catchment using remotely sensed data

Bright Chisadza [a,d,*], Onalenna Gwate [b,e], France Ncube [c], Nkosinathi Moyo [b] and Phibion Chiwara [b]

[a] School of Agriculture, Lupane State University, Private Bag 171, Lupane, Zimbabwe
[b] School of Environment and Development, Lupane State University, Private Bag 171, Lupane, Zimbabwe
[c] School of Environmental and Life sciences, Lupane State University, Private Bag 171, Lupane, Zimbabwe
[d] Faculty of Agriculture, Uganda Martyrs University, P.O. Box 5498 Nkozi Campus, Kampala, Uganda
[e] Afromontane Research Unit and Department of Geography, University of the Free State, South Africa
*Corresponding author. E-mail: brightate@gmail.com

BC, 0000-0003-3343-7455; OG, 0000-0003-0237-4316; FN, 0000-0003-0364-1754; PC, 0000-0002-4148-8204

ABSTRACT

Globally, water is acknowledged as indispensable. It is essential for both human life and environmental needs. However, surface water resources are threatened by human and climatic influences, which may result in changes in size and density. This study aimed to evaluate the effectiveness of the normalised difference water index (NDWI), modified normalised difference water index (MNDWI) and automated water extraction index (AWEI) in detecting land surface water changes using Landsat satellite data. The results showed that the AWEI performed considerably better than the MNDWI and NDWI for extracting water surface area in the Upper Mzingwane sub-catchment, with an overall accuracy of 0.93 and a kappa coefficient of 0.82. The MNDWI and NDWI had overall accuracy/kappa values of 0.88/0.74 and 0.89/0.73, respectively. The AWEI can enhance surface water features while effectively suppressing or eliminating pollution and noise from surrounding vegetation and muddy soil. NDWI/MDWI water information is often mixed with pollution noise, vegetation and muddy soil, overestimating the area of water. All the applied indices indicate a progressive loss in the surface area of the water bodies in the sub-catchment. The decrease in water surface area could be a result of degradation, as it coincided with a decrease in vegetation cover and an increase in degraded areas. Future research needs to investigate the hydrological response of the sub-catchment to the potential influence of climate, variability, change, and land use land cover (LULC) changes.

Key words: remote sensing, surface water changes, Upper Mzingwane sub-catchment, water indices, water resources management

HIGHLIGHTS

- Evaluated performance of three water indices to detect water surface area changes on Landsat satellite data.
- The indices show a progressive loss of surface area of water bodies in the sub catchment from 1990 to 2020.
- The AWEI outperformed MNDWI and NDWI in extracting water surface area, with overall accuracy/kappa coefficient of 0.93/0.82.
- Sub-catchment was undergoing degradation as its ability to retain water deteriorated.

GRAPHICAL ABSTRACT

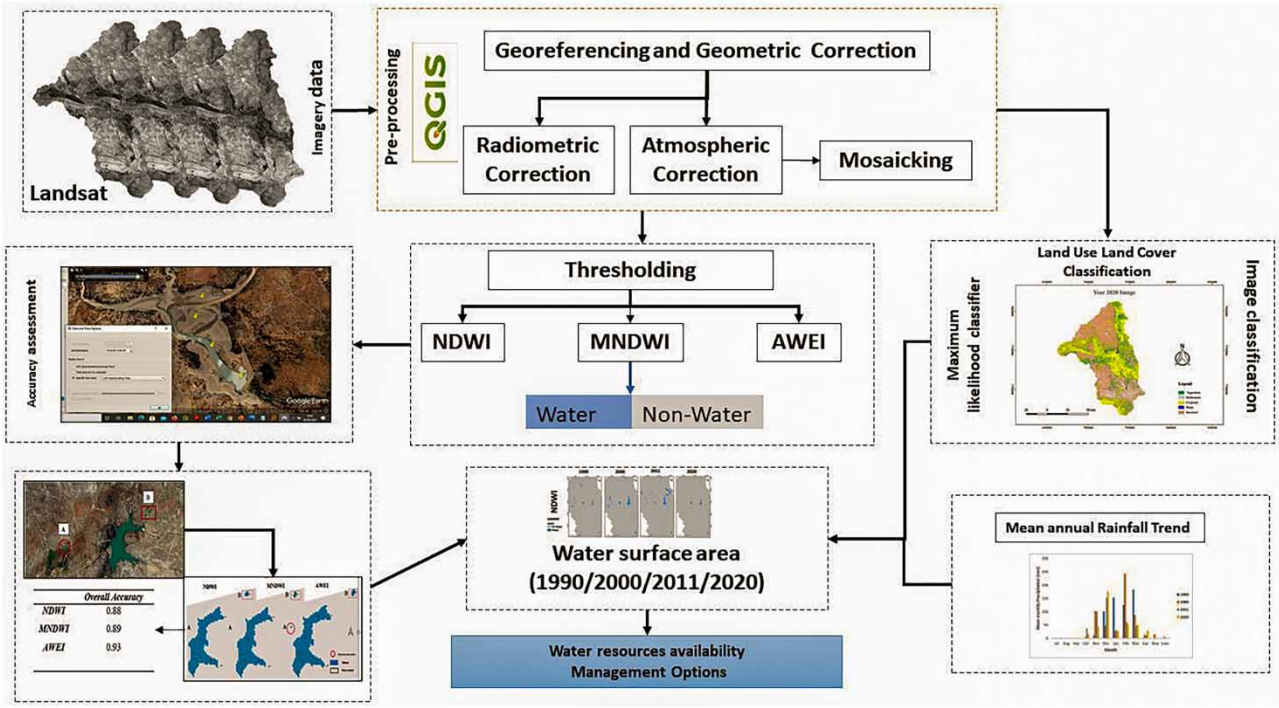

1. INTRODUCTION

Water is essential for the survival of all living things (Gong *et al.* 2020; Herndon *et al.* 2020) and environmental sustainability. Surface water bodies are the most accessible to life. Therefore, surface water bodies should be monitored since they affect nearby human life and ecosystems. Despite their significance, surface water bodies are increasingly susceptible to natural and anthropogenic disturbances (Su *et al.* 2017) owing to increased stresses due to global population expansion and climate change (Cosgrove & Loucks 2015). Natural and man-made disturbances may induce surface water resource shrinkage or expansion (Karpatne *et al.* 2016; Huang *et al.* 2018). Spatiotemporal changes in the surface area of water bodies affect societal socioeconomic development as well as the maintenance of a clean and functional ecosystem. Water volume changes typically have severe effects (Balist *et al.* 2022). For example, a rapid surface water rise may cause floods, while a rapid decline may lead to droughts (Li 2020). Therefore, it is critical to accurately identify surface water, quantify its volume, and monitor its dynamics over time. Consequently, understanding the geographic distribution of surface water resources is important for evaluating and monitoring changes in watersheds and the surrounding environment (Gong *et al.* 2020). Additionally, the ability to detect changes in surface water dynamics and monitor these changes promptly is crucial for policy development and decision-making (Frey *et al.* 2010).

In situ gauge measurements have traditionally been the primary data source for assessing hydrological dynamics. Gauge stations collect data on water level, discharge, and streamflow but not on the spatial dynamics of surface water extent (Li 2020). In most cases, gauge stations are located on major rivers and lakes, but their distribution varies across the world, and their numbers have been decreasing in both developed and developing countries (Shiklomanov *et al.* 2002). Even where gauges exist, legal and institutional constraints often prevent scientific use of the data (Abu-zeid & Shiklomanov 2004). The cost of ground surveys for data collection is also prohibitive. Because of the limited spatial coverage and unavailability of *in situ* observations, assessing changes in water resources is difficult. Remote sensing technology and high-resolution satellite data have made precise surface water mapping and detection possible, particularly in areas where ground data is scarce (Huang *et al.* 2018; Li 2020). Moreover, remote sensing can effectively monitor surface water dynamics. The use of remote sensing is more efficient than *in situ* measurements because it can constantly monitor the Earth's surface at various spatial and temporal dimensions.

This study focused on the application of optical remote sensing in surface water monitoring. The fact that water has a lower reflectance in infrared bands than other land cover categories offer an opportunity for accurate extraction and discrimination of surface water from optical imagery data. Many techniques for obtaining water areas from remotely sensed data exist (e.g. Zhai *et al.* 2015). For example, Frazier & Page (2000) showed that the simplest water extraction method is density slicing of a single infrared band. Surface water can be extracted from land cover maps using supervised or unsupervised categorisation techniques (Yang & Du 2017). In addition, multispectral bands can be used to delineate water using decision trees (Huang *et al.* 2018; Mishra *et al.* 2020). The main drawback of the decision tree technique is that its categorisation criteria are complex to develop and not always universally applicable (Huang *et al.* 2018). Water indices, computed from two or more spectral bands, offer a straightforward and effective technique for extracting water. There are a variety of indices that may be used to estimate surface water areas or the size of a flood. The Tasseled Cap Wetness (TCW) index utilises six channels of surface reflectance data to differentiate water from non-water features (Huang *et al.* 2018). Many researchers have identified water and flood extents using the normalised difference vegetation index (NDVI) (Rokni *et al.* 2014; Acharya *et al.* 2018). NDVI is quite effective in determining aboveground biomass, but it does not help to quickly assess whether surface water extraction is happening (McFeeters 1996). The normalised difference water index (NDWI) and modified normalised difference water index (MNDWI) are considered superior indices for this purpose (McFeeters 1996; Xu 2006). According to Xu (2006), the near-infrared band (NIR) in the NDWI formulae may be substituted with the shortwave infrared band (SWIR), as it is more effective in detecting minor water features. The MNDWI is considered more stable and reliable than the NDWI because it utilises the SWIR band, which is less affected by quantities of sediments and other optically active water components. Thus, the MNDWI has been extensively utilised recently (Huang *et al.* 2018; Gong *et al.* 2020). Feyisa *et al.* (2014) developed the Automated Water Extraction Index (AWEI) using a single threshold. The AWEI is divided into two indices: AWEInsh for no shadows and AWEIsh for differentiating water pixels from shadow pixels. Many recent investigations, for example, Tulbure *et al.* (2016), have used the AWEI to extract water bodies from Landsat imagery. Fisher *et al.* (2016) developed a new water index, WI2015, utilising linear discriminant analysis using surface reflectance on visible, NIR, and SWIR channels.

This research, therefore, utilises remotely sensed data to detect surface water area changes in the Upper Mzingwane subcatchment. The upper Mzingwane contributes 9.3% of the Limpopo River discharge (Maviza & Ahmed 2020) and supplies five of Bulawayo city's potable water supply dams. In addition, upstream and downstream settlements rely on water from this subbasin. The increasing water demand of these settlements and the city of Bulawayo, prolonged droughts and irregular rainfall affect the water supply and lead to water insecurity (Mukuhlani & Nyamupingidza 2014). An improved understanding of water availability in the Upper Mzingwane subbasin is required for sustainable water management.

Climate change is projected to exacerbate water scarcity and increase the frequency and intensity of droughts in catchments (Mann & Gupta 2022). As such, there is a need for more knowledge on the hydrological dynamics of the Upper Mzingwane subbasin to support the design of sustainable water management systems. The Upper Mzingwane subbasin is characterised by recurrent droughts and climate-induced temporal variations in rainfall and runoff, both on an annual and interannual basis (Love *et al.* 2005).

Abimbola *et al.* (2017) and HLPW (2018) reported that collecting climate data in most catchments is difficult, as some areas are not surveyed. Data on climatic and hydrological factors are essential for efficient water resource management (HLPW 2018). The Upper Mzingwane sub-catchment lacks adequate hydrometeorological data. Monitoring and managing water resources is, therefore, a challenge. Current surface water monitoring practices rely on inadequate and unevenly distributed gauging stations in the subbasin.

Furthermore, gauging stations are limited to measuring water depth and discharge and may not be able to adequately detect spatial changes in the water surface. The water surface area is a good metric of the loss of surface water capacity due to sedimentation or climate change. This research, however, has been limited by the availability of data on other hydrological indicators, such as runoff and water quality. Thus, the research only focused on rainfall, land use and surface water area variables.

The study objectives were (a) to evaluate the effectiveness of NDWI, MNDWI, and AWEI in detecting water surface area and (b) to map land surface water in the Upper Mzingwane sub-catchment. The novelty of this work is that it uses a remotely sensed dataset and multiple indices to characterise water surface area changes in a semi-arid inadequately gauged catchment. To the best of our knowledge, this is a relatively new study in Zimbabwe.

2. METHODOLOGY

2.1. Study area description

The Upper Mzingwane Sub-catchment is one of the four sub-catchments of the Mzingwane Catchment of Zimbabwe (Figure 1). Other sub-catchments are Mwenezi, Lower Mzingwane, and Shashe. Located in Zimbabwe's Natural Agro-Ecological Region IV, the Upper Mzingwane sub-catchment spans an area of 2,138 km^2. The sub-catchment receives 450–650 mm of rain annually (Love *et al.* 2010; Maviza & Engelbrecht 2021). The catchment's mean annual runoff is 60 mm per year and flows south into the Limpopo River (Love *et al.* 2006). On an annual basis, the mean lowest and highest temperatures are 5 and 30 °C, respectively, with an estimated potential evaporation gradient of 1,800–2,000 mm (Maviza & Ahmed 2020). The elevation of the Upper Mzingwane sub-catchment varies from 864 to 1,560 m AMSL. The Upper Mzingwane Sub catchment has a diverse land use mix, including agriculture, mining, and urban uses (Maviza & Ahmed 2020).

2.2. Landsat data

The Landsat satellite imagery for April, May, October and November, which coincided with the wet and dry seasons, was obtained from the United States Geological Survey website (http://earthexplorer.usgs.gov/) for the years 1990, 2000, 2011, and 2020. Data from at least two different periods are required to make comparisons when monitoring changes in land use conditions (Alam *et al.* 2020). We selected Landsat images because they are freely available and have relatively moderate resolution considering the size of the study site and our computer capabilities. The selection of these years was based on our

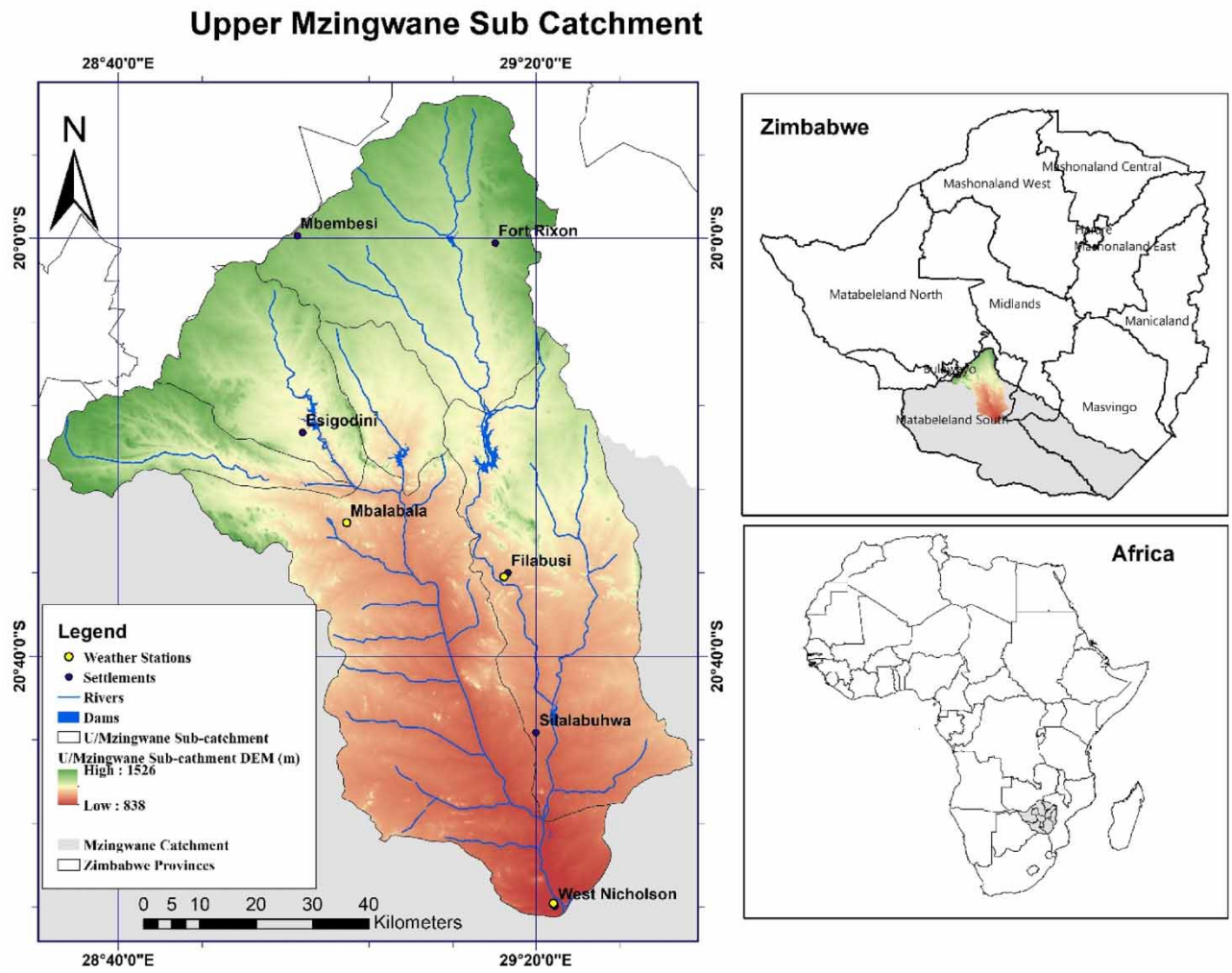

Figure 1 | Upper Mzingwane Subcatchment.

understanding of the history of the catchment. We hypothesised that the fast-track land reform of 2000 had environmental impacts that inadvertently influenced the partitioning of precipitation into various components (Gwate *et al.* 2022). We reckoned that 1990 was representative of the baseline, i.e., the pre-land reform period and subsequent 10-year periods could indicate land use/land cover intensity change due to natural and anthropogenic activities in the catchment. Notably, notwithstanding rapid interventions, land cover change is often a relatively slow process. Table 1 shows the characteristics of the Landsat images selected for the study. The quality of the imagery, scene availability and coverage (Path/row) needed to cover the study area, and cloud cover (<1%) were all aspects taken into consideration when determining the best time periods to use. Consequently, the images for the months of April and May were chosen to represent the end of the growing/wet season when vegetation phenology had fully developed. The images for the months of October and November were also considered as they represented the dry season.

2.3. Image preprocessing

The Semi-Automatic plugin (SCP) in QGIS version 3.4 was used to conduct radiometric calibration and atmospheric correction on the satellite images in preparation for further processing. In doing so, the acquired images were then transformed to at-satellite radiance. Following the conversion to at-satellite radiance, all the images were transformed to at-satellite reflectance. Using the Landsat header files, we extracted the necessary information, such as the date of data collection and sun elevation. Subsequently, the images for each corresponding year period were mosaicked together to produce new images covering the whole sub-catchment. The mosaicking technique, which is based on georeferenced images, was utilised for this purpose. Image coregistration was also applied to ensure geometric alignment for multidate analysis (Stumpf *et al.* 2018).

2.4. Surface water area extraction using the indices

To detect the water surface area changes in the Upper Mzingwane Subcatchment in the period 1990–2020, the NDWI, MNDWI, and AWEI were used to extract water features. The extracted water features were used to compute the total water surface area of the entire sub-catchment. This enabled us to evaluate the effectiveness of NDWI, MNDWI, and AWEI (Table 2) in extracting surface water from Landsat imagery. QGIS version 3.4 was used to compute the NDWI, MNDWI and AWEI and the resulting water surface area of each of the selected dams. In summary, the following stages were involved in the calculation of water surface area based on the indices:

(1) The index algorithm was entered into the raster calculator and executed to generate NDWI, MNDWI and AEWI rasters.
(2) The next step was selecting a threshold and executing the algorithm to distinguish between water and non-water areas.

Table 1 | Characteristics of Landsat data

Satellite	Sensor	Image Scene	Year/Date	Spatial resolution (m)	Cloud Cover	Wavelength (nm)
Landsat-5	TM	171/74 170/74 170/75	1990 05 November	30	0%	Band 1: 450–520 Band 2: 520–600 Band 3: 630–690 Band 4: 760–900 Band 5: 1,550–1,750
Landsat-7	ETM	171/74 170/74 170/75	2000/2011 23 October	30	0%	Band 1: 450–515 Band 2: 525–605 Band 3: 630–690 Band 4: 750–900 Band 5: 1,550–1,750 Band 7: 2,090–2,350.
Landsat-8	OLI	171/74 170/74 170/75	2020 28 October	30	0%	Band 1: 435–451 Band 2: 452–512 Band 3: 533–590 Band 4: 636–673 Band 5: 851–879 Band 6: 1,566–1,651 Band 7: 2,107–2,294 Band 9: 1,363–1,384

Table 2 | Satellite-derived indices used for water feature extraction

Index	Algorithm	Landsat Sensor	Comments	Reference
NDWI	$\text{NDWI} = \frac{(\text{Band 2} - \text{Band 4})}{(\text{Band 2} + \text{Band 4})}$	TM/ETM	Water has a positive value	McFeeters (1996)
	$\text{NDWI} = \frac{(\text{Band 2} - \text{Band 5})}{(\text{Band 2} + \text{Band 5})}$	OLI/TRS		
MNDWI	$\text{MNDWI} = \frac{(\text{Band 2} - \text{Band 5})}{(\text{Band 2} + \text{Band 5})})$	TM/ETM	Water has a positive value	Xu (2006)
	$\text{MNDWI} = \frac{(\text{Band 3} - \text{Band 6})}{(\text{Band 3} + \text{Band 6})}$	OLI/TRS		
AWEI	$AWEI = 4(\text{Band 2} - \text{Band 5}) - (0.25\ \text{Band 4} + 2.75\ \text{Band 7})$		Water has a positive value	Feyisa *et al.* (2014)
	$AWEI = 4(\text{Band 3} - \text{Band 6}) - (0.25\ \text{Band 5} + 2.75\ \text{Band 7})$			

(3) The NDWI, MNDWI and AEWI raster images were converted to polygons using the raster-to-polygon tool.
(4) After selecting and saving water features from the attributes of the generated NDWI, MNDWI and AWEI polygons, the total area of all water bodies was calculated using the open-field calculator.

2.5. Optimum threshold selection

The study applied different threshold values to classify the study area into water and non-water features, as shown in Table 3. To categorise the images into two categories (non-water and water), a manual threshold was applied to each image, according to the methodology used by Rokni *et al.* (2014). The optimum thresholds applied were different for the indices and the wet and dry seasons. The NDWI and MNDWI thresholds are set to zero in the dry months. The AWEI threshold was negative during the rainy months, while the NDWI and MNDWI thresholds were both positive. In rainy months, NDWI, MNDWI, and AWEI had thresholds of 0.15, 0.13, and −0.11, respectively. In both wet and dry months, the AWEI thresholds are lower than the NDWI and MNDWI thresholds.

2.6. Accuracy assessment of the water indices

The efficacy of the indices in extracting surface water area was assessed using an error matrix between referenced surface water bodies and the outcomes of surface water extraction, as described in Zhai *et al.* (2015). This was done to assess the performance of each index in extracting the surface water area. The reference water bodies and non-water sample points were gathered from a high-resolution Google Earth image taken on the same day as the Landsat imagery, which was used to calculate water indices (Figure 2). ArcMap version 10.2 was used to transform the gathered Google Earth sample points to a processing extent corresponding to the water index raster files. Then, the sampled points were transformed into raster images using the point-to-raster function (Zhang *et al.* 2018). Finally, the point raster image (the reference data) was merged with the water index raster picture to provide an output that was utilised to extract the error matrix. Table 4 depicts the error matrix concept used in evaluating accuracy. In Table 4, ***A*** represents the number of correct predictions that an instance is water, ***B*** represents the number of incorrect predictions that an instance is non-water, ***C*** represents the number of incorrect predictions that a pixel is predicted as water, and ***D*** represents the number of correct predictions that an instance is non-water. The results are evaluated using the kappa coefficient and overall accuracy.

Table 3 | Optimum threshold chosen for dry and wet months for the different indices

	Dry months	Wet months
Optimal threshold chosen		
NDWI	0	0.15
MNDWI	0	0.13
AWEI	−0.15	−0.11

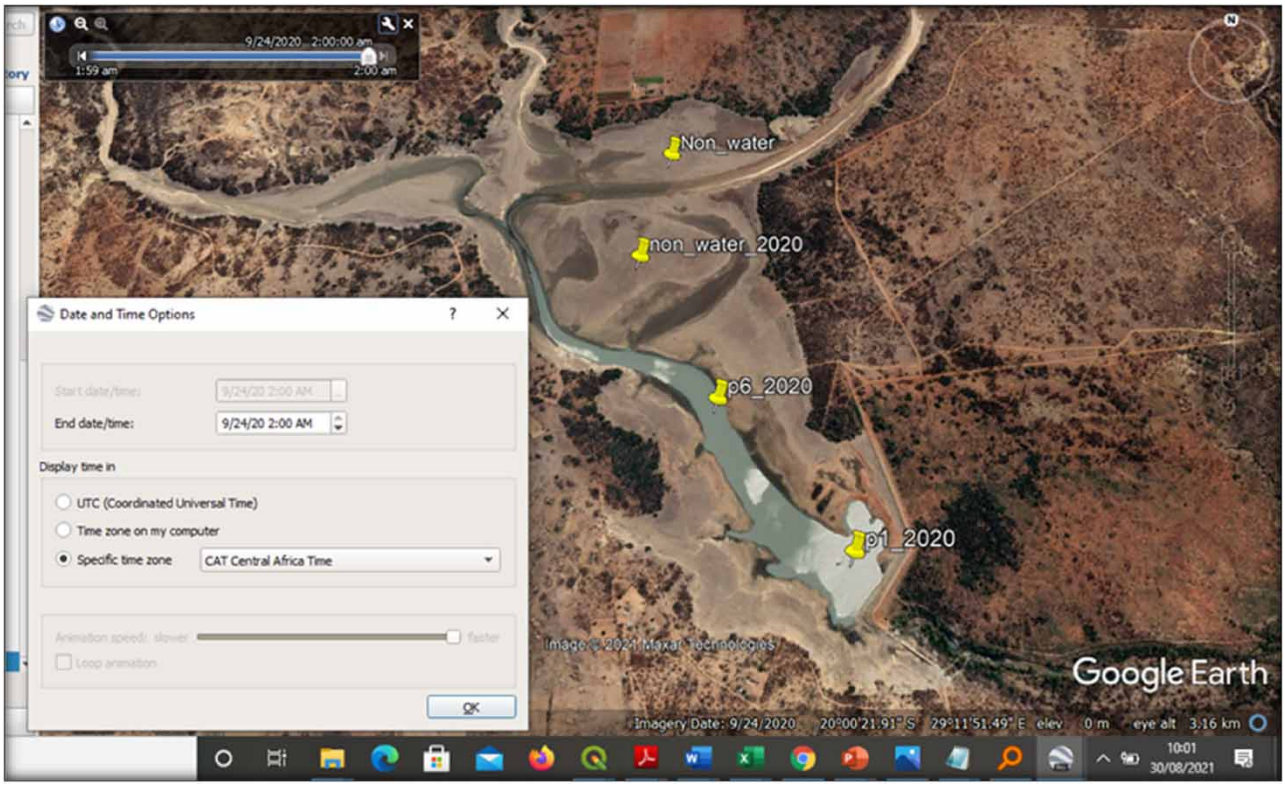

Figure 2 | Sampling of reference data for accuracy assessment.

Table 4 | Error matrix concept

	Index classified image data	
Reference data	**Water**	**Non-Water**
Water	***A***	***B***
Non-Water	***C***	***D***

2.7. Rainfall and runoff data

Rainfall data were acquired from the Meteorological Services Department of Zimbabwe, and the average monthly precipitation was computed for the study years. The rainfall data were subjected to the Mann-Kendall test for trend analysis.

2.8. Land use land cover (LULC) image classification

The supervised classification technique was utilised for image classification using the SCP in QGIS Version 3.4 under the maximum likelihood algorithm. Images were classified based on their digital numbers (DNs) using spectral signatures obtained from training samples (Matlhodi *et al.* 2019). The output classified image was used to create thematic maps. After that, an error matrix was created for the accuracy evaluation of the classified image. Google Earth was used to acquire ground truth data. The classification results were compared to Google Earth-derived ground truth data. Then, classified image results were evaluated using the kappa coefficient, producer accuracy, user accuracy and overall accuracy. Overall, accuracy values between 60 and 99 percent are acceptable, indicating that the accuracy of the LULC classes is within the acceptable range (Matlhodi *et al.* 2019).

3. RESULTS

3.1. Performance of the water indices

The NDWI, MNDWI, and AWEI were evaluated for their efficacies in extracting surface water from Landsat TM, ETM, and OLI TRS data. Some water bodies that were extracted using the NDWI, MNDWI and AWEI are shown in Figure 3, and the extractive capacities of the indices are shown in Figure 4. In Figure 4, the circled water pixel was only identified as water by the AWEI, while the NDWI and MNDWI could not identify the same water pixel for the same place. The AWEI was also able to classify more water pixels for the same water bodies for the areas highlighted as red rectangles in Figure 4, while the NDWI had the least classified water pixels for the same water body. Variations in surface water area extracted over different years using different indices are presented (Figure 5). According to the error matrix, the AWEI had an overall accuracy of 93.1%, a kappa value of 0.82 during the dry season, an overall accuracy of 95%, and a kappa value of 0.89 during the wet season. The MNDWI and the NDWI had dry and wet season kappa values of 0.74/0.82 and 0.73/0.80, respectively (Table 5).

Figure 3 | Satellite imagery showing some water bodies extracted using NDWI, MNDWI and AWEI in Figure 4.

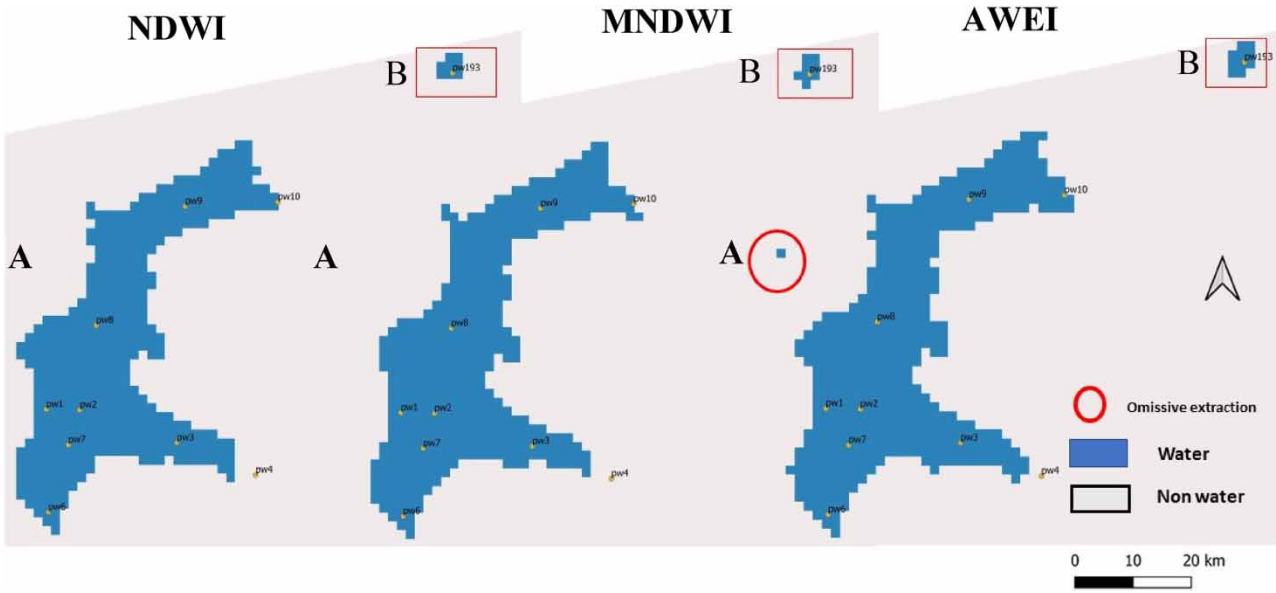

Figure 4 | Comparison of NDWI, MNDWI and AWEI for highlighted water bodies. For 28 October 2020. Please refer to the online version of this paper to see this figure in colour: http://dx.doi.org/10.2166/aqua.2022.089.

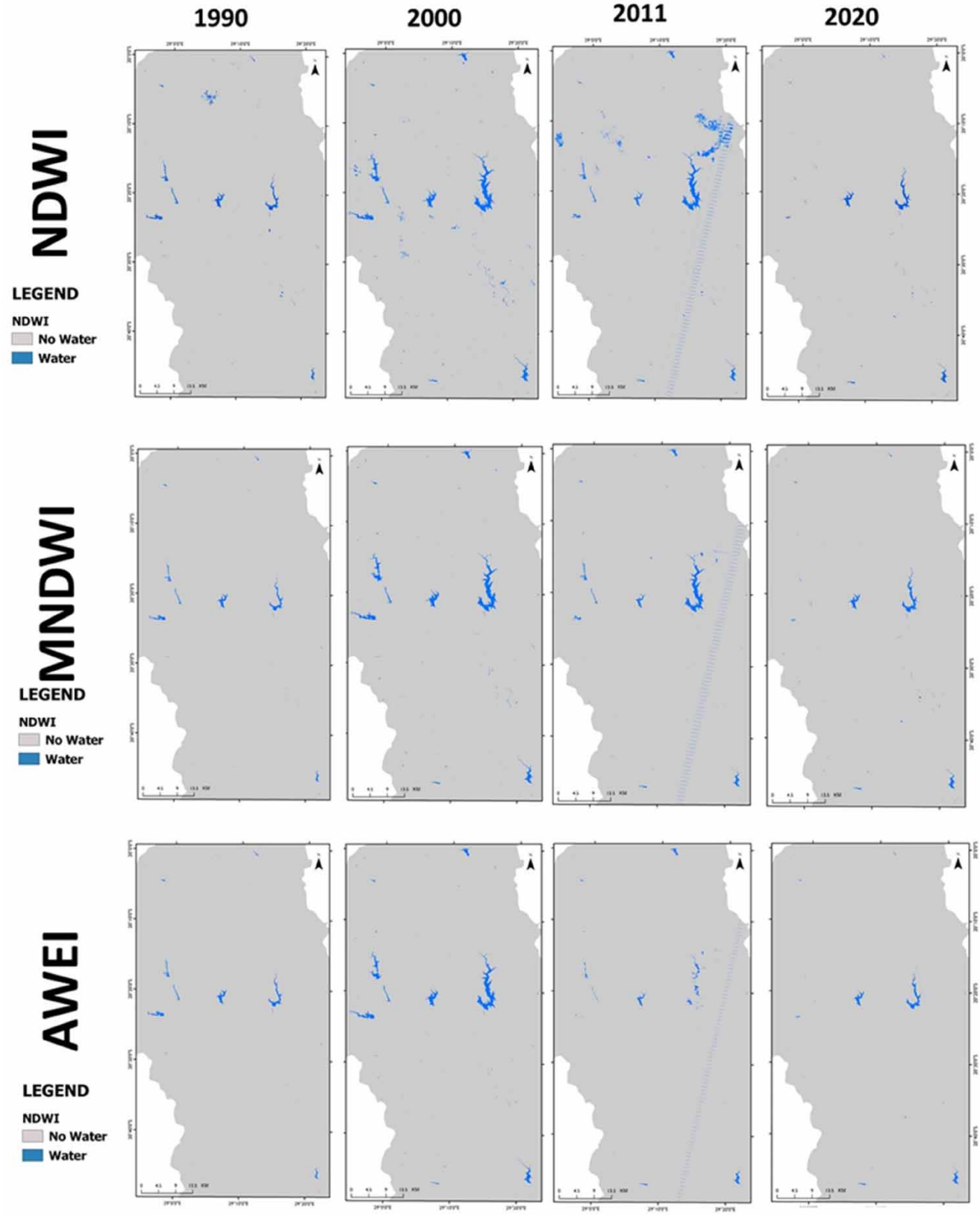

Figure 5 | Variations in water distribution (1990–2020) for parts of the subcatchment based on different indices.

3.2. Water surface area dynamics

The total water surface area increased for all the indices from 1990 to 2000, while there was a decrease in water surface area from 2000 to 2020 for both the wet and dry seasons (Table 6). The total water surface area decreased by 3,309 ha between April 2000 and May 2020 and 2,987 ha between October 2000 and October 2020, which was the worst decline using the NDWI index. The estimated water surface area for some selected dams is shown in Figure 6. The AWEI had the lowest values in water surface area for all the years. The selected dams, Upper Insiza, Insiza, Upper Ncema, Lower Ncema, Mzingwane and Inyankuni, mainly the Bulawayo water supply dams, constituted approximately 67% (NDWI), 86% (MNDWI) and 88% (AWEI) of the total surface water area in the sub-catchment. About 12–33% is covered by small water dams, mainly in the southern parts of the sub-catchment.

3.3. Land use/land cover and rainfall dynamics

3.3.1. Water indices vs. precipitation

Precipitation, one of the most significant variables influencing surface water variations, has the potential to affect the surface water dynamics of the Upper Mzingwane sub-catchment Basin and, as such, should be taken into account. The monthly precipitation in the sub-catchment during the research period is depicted in Figure 7. The precipitation data for 1990 to 2020 showed an increasing trend ($p = 0.003$, tau = 0.31) when subjected to the Mann-Kendall test. February 2000 had the highest mean monthly rainfall (240 mm), and the same year coincided with peak surface water areas in the sub-catchment of approximately 5,562 ha (April) and 4,749 ha (October). Water surface area changes are shown in Figure 9. There were minor variations in the annual precipitation scale throughout the research period, whereas the surface water area experienced more drastic alterations between 1990 and 2000. The changes from 2000 to 2020 were more apparent than those in the previous decade.

The following section attempts to uncover some of the causes for surface water area variations in the Upper Mzingwane sub-catchment by evaluating land use and land cover changes.

3.3.2. LULC accuracy assessment

All of the classified land cover maps were subjected to an accuracy evaluation. The total accuracy of the land cover categorisation varied between 96.68 per cent and 98 per cent. The land cover maps generated Kappa coefficients of 0.93.

3.3.3. LULC vs. water indices

LULC changes over the whole Upper Mzingwane sub-catchment are shown in Figure 8 and Table 7. From 2000 to 2020, the vegetation class covering the sub-catchment decreased from 32 per cent to 11 per cent, indicating a downwards trend in the vegetation coverage. The settlements and cropland increased between 2000 and 2011 but then declined, as shown in Table 6. Bare/degraded land increased significantly in 2020, accounting for 47 per cent of the entire

Table 5 | Accuracy assessment of applied indices

	Dry Season		Wet Season	
	Overall Accuracy	Kappa Coefficient (k)	Overall Accuracy	Kappa Coefficient (k)
NDWI	0.88	0.73	0.93	0.80
MNDWI	0.89	0.74	0.94	0.82
AWEI	0.93	0.82	0.95	0.89

Table 6 | Estimated water surface area for the Upper Mzingwane sub-catchment

		06-May-90	05-Nov-90	23-Apr-00	23-Oct-00	14-Apr-11	23-Oct-11	24-May-20	28-Oct-20
					Area (ha)				
Water Index	NDWI	2,154	1,592	5,562	4,749	4,279	3,890	2,253	1,762
	MNDWI	2,127	1,481	4,693	4,531	3,086	2,805	1,962	1,760
	AWEI	2,204	1,424	5,171	3,935	1,473	1,339	1,820	1,666

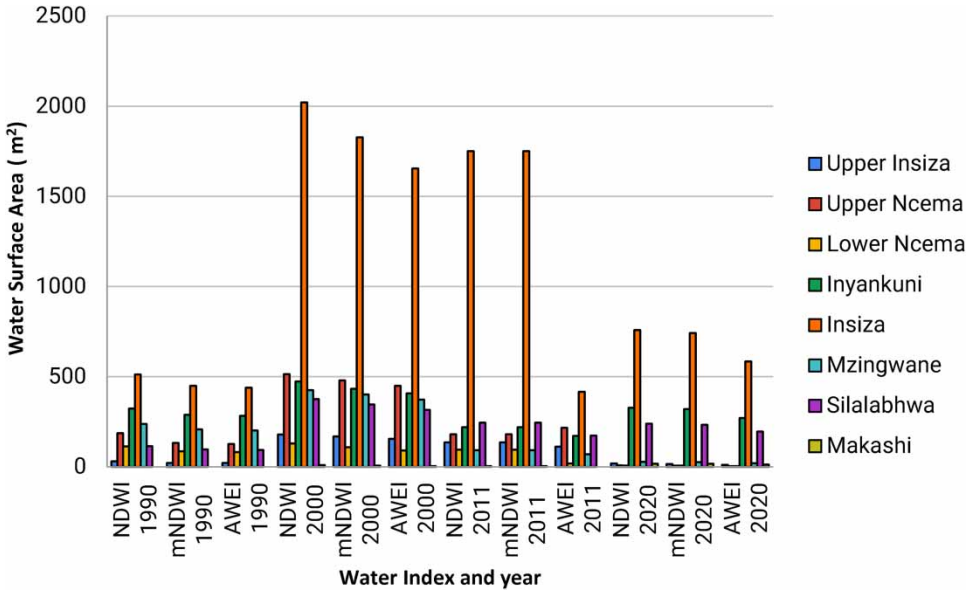

Figure 6 | Variation in water surface area for the selected dams for 1990, 2000, 2011 and 2020 using different indices.

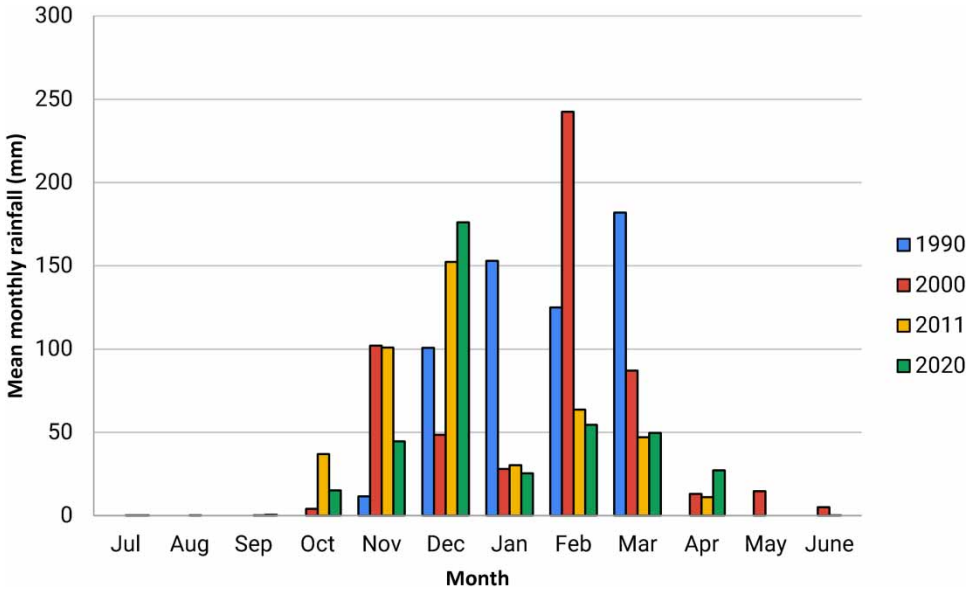

Figure 7 | Monthly precipitation variation over the study period.

sub-catchment area. Between 2000 and 2011, the total water area fell from 6,129 ha to 4,290.31 ha and dropped to 3,956.58 in 2020.

3.3.4. Land cover land use (LULC), rainfall and surface water area dynamics

The mean water surface area determined from the water index results was compared with the total annual precipitation contribution for each study year and the LULC images (Table 8 and Figure 9). The mean monthly water surface area in the wet months decreased from 5,142 m^2 to 2,012 m^2, while it decreased by 4,405 m^2 to 1,729 m^2 in the dry season between 2000 and 2020. The LULC and index techniques showed that the water area decreased from 2000 to 2020.

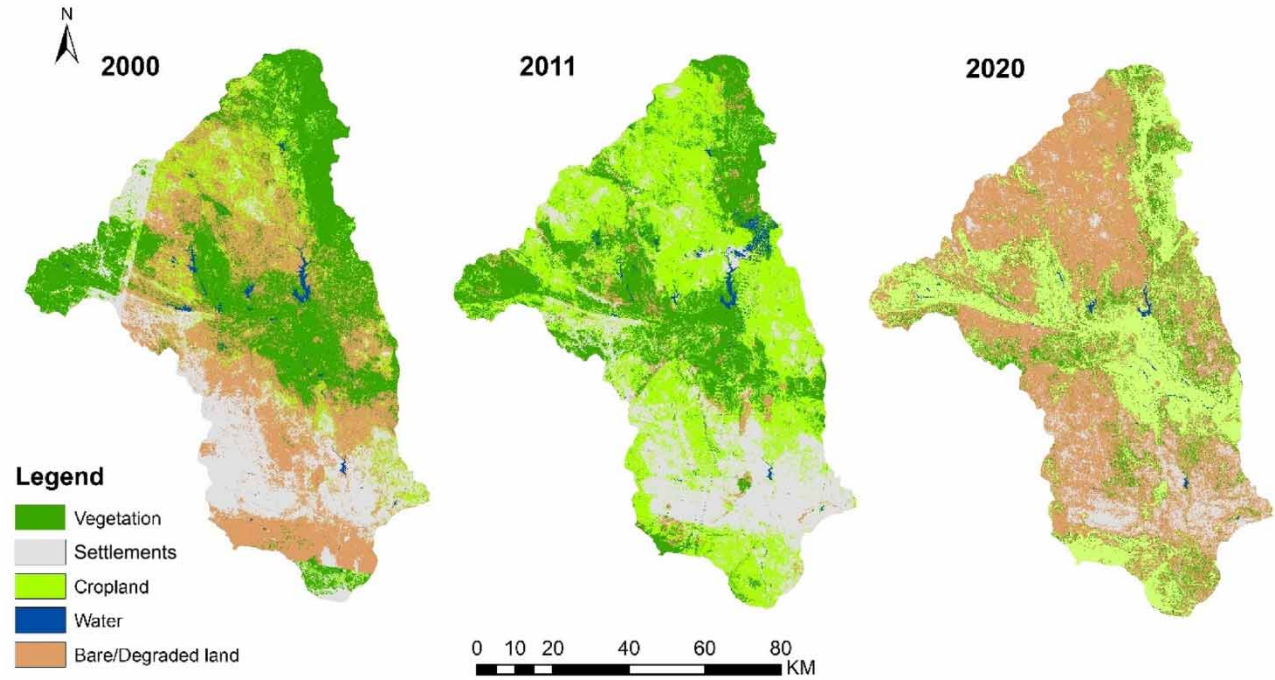

Figure 8 | LULC images for the Upper Mzingwane subcatchment.

Table 7 | LULC area changes

Land Cover type / Year	Area Covered (Ha)		
	2000	2011	2020
Vegetation	239,068.89	199,180.53	84,137.04
Settlements (Homesteads and Built-up area)	154,028.3	183,379.4	66,621.06
Cropland	94,798.35	316,405.3	231,941.2
Water	6,129	4,290.31	3,956.58
Bare/Degraded land	241,161.6	276,490.53	348,532.2

4. DISCUSSION

4.1. Performance of indices

Remote sensing is critical in providing spatially explicit information in the context of a paucity of observed data. However, this information is generated by models and may not necessarily reproduce reality at all times, but validations have proven that such data were still valuable. Hence, we believe that the data generated in this manuscript could reflect reality, and our results are valid. The indices had various thresholds. NDWI and MNDWI thresholds were set to 0 during the dry season. The NDWI and MNDWI thresholds for the wet season were 0.15 and 0.13, respectively. AWEI threshold values were below zero. According to (Zhai *et al.* 2015), optimal thresholds for water indices rely on subpixel water and non-water element ratios. The optimum threshold values are determined by the environmental features of the research location, such as terrain and shadows, as well as other factors (Ji *et al.* 2009).

The current study demonstrates that the AWEI performed considerably better than the MNDWI and NDWI for extracting water surface area in the Upper Mzingwane sub-catchment since the former yielded relatively higher accuracies. The sub-catchment has both rural and urban settlements. As such, near urban setups, some buildings could result in shadows and

Table 8 | Mean wet and dry months water surface area and variability with LULC and precipitation

	LULC Map 1990		LULC Map 2000		LULC Map 2011		LULC Map 2020	
Parameter	**Wet Months 06-May-90**	**Dry Months 05-Nov-90**	**Wet Months 23-Apr-00**	**Dry Months 23-Oct-00**	**Wet Months 14-Apr-11**	**Dry Months 23-Oct-11**	**Wet Months 24-May-20**	**Dry Months 28-Oct-20**
Water surface Area (m^2)	2,162	2,249	5,142	4,405	2,946	2,678	2,012	1,729
Annual rainfall (mm)	573		545		442		393	
LULC water class (m^2)	4,000		6,129		4,290.31		3,956.58	

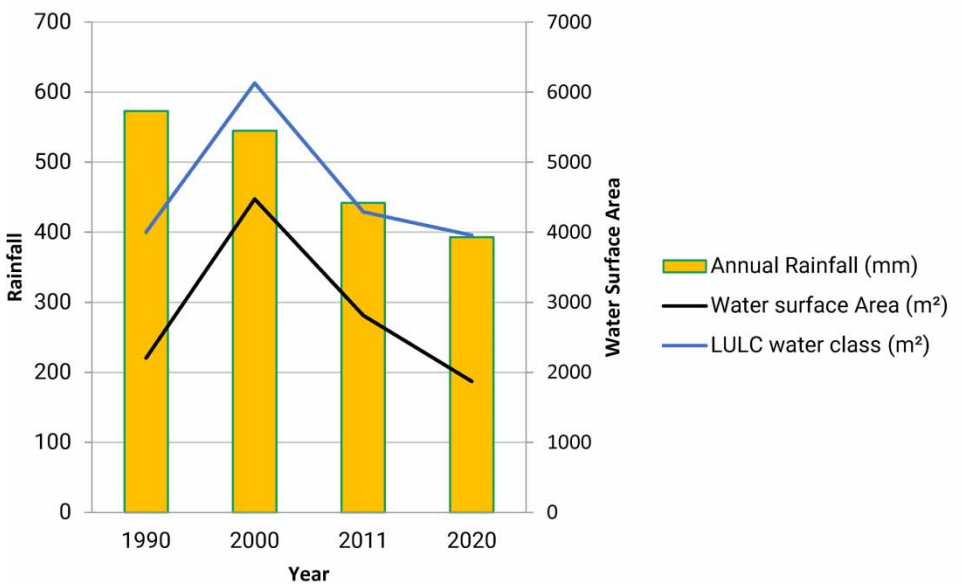

Figure 9 | Association between Figure 6 selected dam water surface area, LULC water class and annual rainfall in the Upper Mzingwane sub-catchment (1990–2020).

high reflectance from bare ground, thus affecting the imagery. According to Zhai *et al.* (2015), the AWEI can distinguish water features from shadows and high-albedo geographic features compared to the MDWI and NDWI. The MNDWI performed relatively the same as NDWI, with dry season overall accuracy/kappa values of 0.88/0.74 and 0.89/0.73, respectively, indicating a marginal difference between the two indices. The wet season results showed the same marginal difference between NDWI and MDWI, with overall accuracy/kappa values of 0.93/0.80 and 0.94/0.82, respectively. These values are comparable with those found by Zhai *et al.* (2015). Overall, the performance of the indices achieved better accuracy during the wet season than during the dry season. This could be due to the high depth of water in the water bodies because of more water during the wet season, resulting in improved water pixel values.

In contrast, the lower performance of indices in the dry season could be due to enhanced pollution and the presence of suspended matter during the late dry season, which reduces the contrast between water and the surrounding muddy sections. However, small water bodies and shallow streams could not be fully retrieved (in terms of shape and extent) from Landsat images; thus, the model's results are not very excellent in extracting water from small water bodies. This may be due to the spatial resolution of Landsat, which makes it impossible to accurately estimate the area of shallow and smaller water bodies less than 1 hectare in size.

The performance of the three indicators applied in this study was satisfactory. This is in agreement with Buma *et al.* (2018), who found that water detection techniques are useful for evaluating and comparing surface water resources from year to year. In addition, according to Zhai *et al.* (2015), the optimum index is determined by the research location's environmental features, including terrain and shadows. In this research, however, none of the three indices used were able to discriminate water

edges, very small dams and ponds effectively. This may be due to the Landsat imagery spatial resolution of 30 m × 30 m, which is likely to result in mixed pixels for shallow and small dams. A similar observation was made by Kaptué *et al.* (2013), who observed that spectral confusion caused by fluctuations in water depth and turbidity as well as the poor spatial resolution may interfere with water clarity and that thresholds may erroneously classify surfaces as land rather than water.

Furthermore, changes in the sun's angle and the composition of the atmosphere and water bodies' biophysical and chemical properties may influence water's reflectance (Frazier & Page 2000; Huang *et al.* 2018; Herndon *et al.* 2020). NDWI had the lowest overall accuracy compared to AWEI and MNDWI. This is consistent with Campos *et al.* (2012), who argued that NDWI may fail to distinguish between built-up regions from some land cover classes, such as sand, which may all seem like water features (Campos *et al.* 2012). Similarly, MNDWI, another widely used technique of surface water identification, frequently mistook vegetated regions for bodies of water (Kaptué *et al.* 2013). This is a well-documented problem resulting from the inability of the MNDWI to differentiate between vegetation and flooded vegetation or vegetated water; therefore, these could have also been the reasons for the poor performance of both the NDWI and MDWI compared to the AWEI.

4.2. Surface water area dynamics

The dynamics of surface water depict significant variation during the study period. Between 1990 and 2000, the indices revealed a rise in the water surface area in the Upper Mzingwane sub-catchment. This could have been indicative of a significant increase in rainfall and in the number of water bodies constructed in the sub-catchment between 1990 and 2000. However, there is also a need to evaluate other underlying causes that have contributed to surface water alterations that occurred from 1990 to 2000, prior to the implementation of land reform in the Upper Mzingwane sub-catchment, and those that took place during the following two decades (2000–2020). The increase in water surface area during the wet seasons may be ascribed to wet season rainfall for all the years. The same observation was made by Anguo (2011), who noted that precipitation accounts for 50%–55% of surface water area changes during the wet season. In addition, there was less water abstraction over this period of time because of less population, among other factors (Mutsvangwa 2002; Baker 2012). According to the research findings, the Upper Mzingwane sub-catchment lost more than half of its water surface area between 2000 and 2020. The LULC dynamics showed a decrease in vegetation cover and an increase in degraded areas in the post-land reform period, which coincided with the decrease in water surface area. The observed loss of water surface area in the Upper Mzingwane sub-catchment could be due to the changes in LULC conditions in the post-land reform period. Comparison with other studies, for example, Rokni *et al.* (2014) and Karpatne *et al.* (2016), reveals that surface water bodies are dynamic in character and may shrink or increase due to human or naturally driven behaviour causes. The storage capacity of the dams in the Upper Mzingwane sub-catchment may continue to decline if the current trend of shrinking water surface area continues. Reducing degradation could go a long way in improving water retention in the sub-catchment. This is very important since the dams offer many advantages to the community and the people who live in the surrounding areas, especially Bulawayo, and it is imperative that they be protected. As a result, policymakers must take adequate steps to avoid future declines in the dam surface area while restoring the dams' surface area to their former conditions. Land use, land cover, and extended periods of drought can decrease the dams' surface area under consideration.

4.3. Implications of surface water changes on water resource availability and water resource management

The main findings from the current study indicate that the selected set of indices can be effectively used in mapping and monitoring spatiotemporal water dynamics in the sub-catchment and can inform water management decisions. This is in line with Buma *et al.* (2018), who stated that constant monitoring of spatiotemporal surface water distribution could provide information on surface water dynamics from which water management strategies can be drawn. The present study provided evidence that the surface water resources in the Upper Mzingwane sub-catchment experienced a significant decrease over the years, particularly during the dry season. Consequently, available water is not able to satisfy demand from competing uses and users, especially during late dry seasons, resulting in water shortages (late September, October and November) (Mutsvangwa 2002). It would be necessary to more thoroughly examine the underlying causes of the decline in water surface area as a first step toward reversing this situation. Furthermore, land use and land cover patterns have shifted, with a distinct decrease in natural vegetation cover and increase cultivated and degraded land across the sub-catchment.

The Mann-Kendall test indicates that the general trend in rainfall increased between 1990 and 2020. This would imply an increase in water surface area as well as an increase in catchment yield. However, the water indices, on the other hand, show a progressive reduction in the water surface area of the sub-catchment water bodies, indicating that the catchment could be

undergoing degradation. However, comprehensive research aimed at understanding the hydrological response of the sub-catchment to these problems will be of critical significance in improving our understanding of the system. Understanding these variations in surface water can help identify the best solutions to serious problems such as drought, flooding, siltation and water scarcity, and there is a need to develop the best possible integrated water resource strategy or measures that take into account both the supply and demand sides of the water equation. Another aspect worth investigating is the degree to which water allocation in the sub-catchment takes into account spatiotemporal changes in the hydrological processes that directly impact water availability. This research shows that approximately 67–88% of surface water in the sub-catchment is found in the major reservoirs that provide the city of Bulawayo with potable water. These major dams are mostly situated in the northern parts of the sub-catchment. This means that the rest of the surface water in the subbasin (approximately 12–33%) is found in small dams, rivers and ponds. Therefore, the water accessible to rural farmers in the sub-catchment to meet their needs, such as potable water supply and agricultural and mining needs, is found in these small dams, rivers and ponds, which constitute 12–33% of the total sub-catchment surface water supplies. Consequently, a better understanding of how much water is contributed by the major dams to local communities in the Upper Mzingwane is also needed.

5. CONCLUSION

Our findings demonstrated that all the models used in this study can successfully extract information about surface water bodies to a larger extent and may be used to monitor dynamic changes in surface water. We also conclude that the Landsat TM, ETM, and OLI TRS images are suitable for extracting surface water using the NDWI, MNDWI, and AWEI methods. Compared to a water body's classification findings, the AWEI algorithms are more accurate at extracting surface water information than the other techniques due to the high classification accuracies in this study. Hence, our results suggest that the AWEI technique is the most effective method for identifying water bodies and detecting surface water in the research area.

The decrease in vegetation cover accompanied by an increase in degraded land in a context of increasing precipitation could have led to a decline in the surface water area. This suggests that the catchment was undergoing degradation as its ability to retain water deteriorated. The reduction in dam water surface areas implies that the storage capacity of the dams in the Upper Mzingwane sub-catchment could also decline, compounding water supply problems in the catchment. Hence implementing schemes that improve water retention in the catchment will be critical.

6. RECOMMENDATIONS

Based on the findings, the study recommends the following:

(1) Future studies must take advantage of publicly accessible high-resolution data sources to improve the accuracy of indices such as sentinel data to monitor the health of tiny water bodies with a surface area of less than 1 ha.
(2) Examine the underlying causes of the reported decline in water surface area in the Upper Mzingwane subcatchment as a first step towards reversing this situation.
(3) The degree to which water allocation in the subcatchment takes into account spatiotemporal changes in the hydrological processes that directly impact water availability is another aspect that has to be investigated.
(4) Apply other indicators such as temperature, water quality, etc., in the analysis.

DATA AVAILABILITY STATEMENT

All relevant data are included in the paper or its Supplementary Information.

CONFLICT OF INTEREST

The authors declare there is no conflict.

REFERENCES

Abimbola, O. P., Wenninger, J., Venneker, R. & Mittelstet, A. R. 2017 The assessment of water resources in ungauged catchments in Rwanda. *Journal of Hydrology: Regional Studies* **13**, 274–289. https://doi.org/10.1016/j.ejrh.2017.09.001.

Abu-zeid, M. & Shiklomanov, I. A. 2004 *Water Resources as A Challenge for the 21st Century*, No. 152. World Meteorological Organisation (WMO), Geneva.

Acharya, T. D., Subedi, A. & Lee, D. H. 2018 Evaluation of water indices for surface water extraction in a landsat 8 scene of Nepal. *Sensors (Switzerland)* **18** (8), 1–15. https://doi.org/10.3390/s18082580.

Alam, A., Bhat, M. S. & Maheen, M. 2020 Using Landsat satellite data for assessing the land use and land cover change in Kashmir valley. *GeoJournal* **85** (6), 1529–1543. https://doi.org/10.1007/s10708-019-10037-x.

Anguo, M. 2011 The Variation Characteristic of Rainfall of Qingjiang River Basin under the Global Climate Warming. *Undefined*.

Baker, J. 2012 Water supply challenges in Bulawayo, Zimbabwe GIS in water resources. *Water Resources*. Available from: http://www.ce.utexas.edu/prof/maidment/giswr2012/TermPaper/Baker.pdf (accessed 17 April 2017).

Balist, J., Malekmohammadi, B., Jafari, H. R., Nohegar, A. & Geneletti, D. 2022 Detecting land use and climate impacts on water yield ecosystem service in arid and semi-arid areas. A study in Sirvan River Basin-Iran. *Applied Water Science* **12** (1), 4. https://doi.org/10.1007/s13201-021-01545-8.

Buma, W. G., Lee, S. I. & Seo, J. Y. 2018 Recent surface water extent of lake Chad from multispectral sensors and GRACE. *Sensors (Switzerland)* **18** (7). https://doi.org/10.3390/s18072082.

Campos, J. C., Sillero, N. & Brito, J. C. 2012 Normalised difference water indexes have dissimilar performances in detecting seasonal and permanent water in the Sahara–Sahel transition zoneitle. *Journal of Hydrology*. https://doi.org/10.1016/j.jhydrol.2012.07.042.

Cosgrove, W. J. & Loucks, D. P. 2015 Water management: current and future challenges and research directions. *Water Resources Research* **51** (6), 4823–4839. https://doi.org/10.1002/2014WR016869.

Feyisa, G. L., Meilby, H., Fensholt, R. & Proud, S. R. 2014 Automated water extraction index: a new technique for surface water mapping using Landsat imagery. *Remote Sensing of Environment* **140**, 23–35. https://doi.org/10.1016/J.RSE.2013.08.029.

Fisher, A., Flood, N. & Danaher, T. 2016 Comparing Landsat water index methods for automated water classification in eastern Australia. *Remote Sensing of Environment* **175**, 167–182. https://doi.org/10.1016/j.rse.2015.12.055.

Frazier, P. S. & Page, K. J. 2000 Water body detection and delineation with Landsat TM data. *Photogrammetric Engineering and Remote Sensing* **66** (12), 1461–1467.

Frey, H., Huggel, C., Paul, F. & Haeberli, W. 2010 Automated detection of glacier lakes based on remote sensing in view of assessing associated hazard potentials. *Grazer Schriften der Geographie und Raumforschung* **45**, 261–272. doi:10.5167/UZH-128917.

Gong, W., Liu, T., Jiang, Y. & Stott, P. 2020 Applicability of the surface water extraction methods based on China's GF-2 HD satellite in Ussuri River, Tonghe County of Northeast China. *Nature Environment and Pollution Technology* **19** (4), 1537–1545. https://doi.org/10.46488/NEPT.2020.v19i04.020.

Gwate, O., Dube, H., Sibanda, M., Dube, T., Chisadza, B. & Nyikadzino, B. 2022 Understanding the influence of land cover change and landscape pattern change on evapotranspiration variations in Gwayi catchment of Zimbabwe. *Geocarto International* 1–17. https://doi.org/10.1080/10106049.2022.2032386.

Herndon, K., Muench, R., Cherrington, E. & Griffin, R. 2020 An assessment of surface water detection methods for water resource management in the Nigerien Sahel. *Sensors (Switzerland)* **20** (2), 1–14. https://doi.org/10.3390/s20020431.

HLPW 2018 An agenda for water action: high-level panel on water outcome document. In: *Making Every Drop Count*. Available from: https://sustainabledevelopment.un.org/content/documents/17825HLPW_Outcome.pdf

Huang, C., Chen, Y., Zhang, S. & Wu, J. 2018 Detecting, extracting, and monitoring surface water from space using optical sensors: a review. *Reviews of Geophysics* **56** (2), 333–360. https://doi.org/10.1029/2018RG000598.

Ji, L., Zhang, L. & Wylie, B. 2009 *Astermndwi2009_Nov_1307*-1317. *75*(11), 1307–1317.

Kaptué, A. T., Hanan, N. P. & Prihodko, L. 2013 Characterisation of the spatial and temporal variability of surface water in the Soudan-Sahel region of Africa. **118** (November), 1472–1483. https://doi.org/10.1002/jgrg.20121.

Karpatne, A., Khandelwal, A., Chen, X., Mithal, V., Faghmous, J. & Kumar, V. 2016 Global monitoring of inland water dynamics: state-of-the-art, challenges, and opportunities. *Studies in Computational Intelligence* **645**, 121–147. https://doi.org/10.1007/978-3-319-31858-5_7.

Li, L. 2020 *Satellite-based monitoring of surface water dynamics*. doi:10.3990/1.9789036549417.

Love, D., Taigbenu, A. & Jonker, L. 2005 An overview of the Mzingwane Catchment, a contribution to the WaterNet Challenge Program Project 17 'Integrated Water Resource Management for Improved Rural Livelihoods : Managing risk, mitigating drought and improving water productivity in the water s. *Management*, *February*, 1–20.

Love, D., Uhlenbrook, S., Madamombe, E., Twomlow, S. & van der Zaag, P. 2006 An evaluation of climate and runoff variability and associated livelihood risks in the Mzingwane. May. Available from: https://www.academia.edu/20386955/AN_EVALUATION_OF_CLIMATE_AND_RUNOFF_VARIABILITY_AND_ASSOCIATED_LIVELIHOOD_RISKS_IN_THE_MZINGWANE_CATCHMENT_LIMPOPO_BASIN_ZIMBABWE

Love, D., Uhlenbrook, S., Twomlow, S. & van Der Zaag, P. 2010 Changing hydroclimatic and discharge patterns in the northern Limpopo Basin, Zimbabwe. *Water SA* **36** (3), 335–350. Available from: http://www.scielo.org.za/scielo.php?script=sci_arttext&pid=S1816-79502010000300015

Mann, R. & Gupta, A. 2022 Temporal trends of rainfall and temperature over two sub-divisions of Western Ghats. *HighTech and Innovation Journal* **3**, 28–42. https://doi.org/10.28991/hij-sp2022-03-03.

Matlhodi, B., Kenabatho, P. K., Parida, B. P. & Maphanyane, J. G. 2019 Evaluating land use and land cover change in the Gaborone dam catchment, Botswana, from 1984-2015 using GIS and remote sensing. *Sustainability (Switzerland)* **11** (19). https://doi.org/10.3390/su11195174

Maviza, A. & Ahmed, F. 2020 Analysis of past and future multi-temporal land use and land cover changes in the semi-arid Upper-Mzingwane sub-catchment in the Matabeleland south province of Zimbabwe. *International Journal of Remote Sensing* **41** (14), 5206–5227. https://doi.org/10.1080/01431161.2020.1731001.

Maviza, A. & Engelbrecht, F. 2021 Twentieth century precipitation trends in the Upper Mzingwane Sub-catchment of the Northern Limpopo Basin, Zimbabwe. *Preprints* 1–25. https://doi.org/https://doi.org/10.21203/rs.3.rs-350963/v1.

McFeeters, S. K. 1996 The use of the Normalised Difference Water Index (NDWI) in the delineation of open water features. *International Journal of Remote Sensing* **17** (7), 1425–1432. https://doi.org/10.1080/01431169608948714.

Mishra, V., Limaye, A. S., Muench, R. E., Cherrington, E. A. & Markert, K. N. 2020 Evaluating the performance of high-resolution satellite imagery in detecting ephemeral water bodies over West Africa. *International Journal of Applied Earth Observation and Geoinformation* **93** (August), 102218. https://doi.org/10.1016/j.jag.2020.102218.

Mukuhlani, T. & Nyamupingidza, M. T. 2014 Water scarcity in communities, coping strategies and mitigation measures: the case of Bulawayo. *Journal of Sustainable Development* **7** (1). https://doi.org/10.5539/jsd.v7n1p144.

Mutsvangwa, C. 2002 Management of water resources in Buluwayo city. In: *People and Systems for Water, Sanitation and Health: Proceedings of the 27th WEDC Conference*. pp. 249–251.

Rokni, K., Ahmad, A., Selamat, A. & Hazini, S. 2014 Water feature extraction and change detection using multitemporal landsat imagery. *Remote Sensing* **6** (5), 4173–4189. https://doi.org/10.3390/rs6054173.

Shiklomanov, A. I., Lammers, R. B. & Vörösmarty, C. J. 2002 Widespread decline in hydrological monitoring threatens Pan-Arctic research. *Eos* **83** (2). https://doi.org/10.1029/2002EO000007

Stumpf, A., Michéa, D. & Malet, J.-P. 2018 Improved Co-Registration of sentinel-2 and landsat-8 imagery for earth surface motion measurements. *Remote Sensing* **10** (2), 160. https://doi.org/10.3390/rs10020160.

Su, Z., He, Y., Dong, X. & Wang, L. 2017 *Drought Monitoring and Assessment Using Remote Sensing*. Springer, Cham, pp. 151–172. https://doi.org/10.1007/978-3-319-43744-6_8

Tulbure, M. G., Broich, M., Stehman, S. V. & Kommareddy, A. 2016 Surface water extent dynamics from three decades of seasonally continuous Landsat time series at subcontinental scale in a semi-arid region. *Remote Sensing of Environment* **178**, 142–157. https://doi.org/10.1016/J.RSE.2016.02.034.

Xu, H. 2006 Modification of normalised difference water index (NDWI) to enhance open water features in remotely sensed imagery. *International Journal of Remote Sensing* **27** (14), 3025–3033. https://doi.org/10.1080/01431160600589179.

Yang, J. & Du, X. 2017 An enhanced water index in extracting water bodies from Landsat TM imagery. **23** (3), 141–148. https://doi.org/10.1080/19475683.2017.1340339.

Zhai, K., Wu, X., Qin, Y. & Du, P. 2015 Comparison of surface water extraction performances of different classic water indices using OLI and TM imageries in different situations. **18** (1), 32–42. https://doi.org/10.1080/10095020.2015.1017911. Available from: Http://Www.Tandfonline.Com/Action/JournalInformation?Show=a*imsScope&journalCode = tgsi20#.VsXpLiCLRhE*

Zhang, F., Li, J., Zhang, B., Shen, Q., Ye, H., Wang, S. & Lu, Z. 2018 A simple automated dynamic threshold extraction method for the classification of large water bodies from landsat-8 OLI water index images. *International Journal of Remote Sensing* **39** (11), 3429–3451. https://doi.org/10.1080/01431161.2018.1444292.

First received 9 May 2022; accepted in revised form 26 September 2022. Available online 5 October 2022